



## In(Ga)As/GaAs quantum dots grown on a (111) surface as ideal sources of entangled photon pairs

Andrei Schliwa,\* Momme Winkelkemper, Anatol Lochmann, Erik Stock, and Dieter Bimberg  
*Institut für Festkörperphysik, Technische Universität Berlin, Hardenbergstr. 36, 10623 Berlin, Germany*

(Received 23 September 2009; published 21 October 2009)

Self-organized In(Ga)As/GaAs quantum dots (QDs) grown on (111) substrate are proposed as ideal sources for the generation of entangled photon pairs. Due to the threefold rotational symmetry of the (111) surface, QDs with  $C_{3v}$  symmetry or higher are expected to develop during growth. In contrast to QDs on (001)-oriented substrates, the symmetry of the confinement potential of (111) QDs is not lowered by piezoelectric effects. As a result the excitonic bright splitting vanishes and the biexciton  $\rightarrow$  exciton  $\rightarrow 0$  recombination cascade can be used for the generation of entangled photons. We evaluate the spectroscopic separability of excitonic and biexcitonic emissions as a function of QD size, shape, and composition using the configuration-interaction model in conjunction with eight-band  $\mathbf{k}\cdot\mathbf{p}$  theory. The piezoelectric field in (111) QDs predominantly aligns along the growth direction and gives rise to vertical charge separation. First- and second-order piezoelectric fields are oriented in opposite directions. The In/Ga ratio inside the QD determines the leading contribution and can be employed to balance both terms in order to achieve a field-free situation with maximal electron-hole overlap. The biexciton binding energy depends on the net piezoelectric potential drop across the QD vertical extension and becomes maximal if the first- and second-order fields outweigh each other within the QD interior.

DOI: [10.1103/PhysRevB.80.161307](https://doi.org/10.1103/PhysRevB.80.161307)

PACS number(s): 73.21.La

In this work we evaluate the (111)-substrate orientation for quantum dot (QD) growth to obtain a source of entangled photon pairs.<sup>1</sup> Such sources, preferably electrically driven, are essential for a number of protocols of future secure communication systems employing quantum key distribution.<sup>2,3</sup> Resonant-cavity light-emitting diodes based on QDs are ideal candidates for such devices, because they combine atomlike properties with the opportunity of electrical charge injection.

The creation of entangled photon pairs in QD-based sources relies on the biexciton ( $XX$ )  $\rightarrow$  exciton ( $X$ )  $\rightarrow 0$  recombination cascade.<sup>4</sup> A vanishing fine-structure splitting (fss) of the exciton bright state is essential in order to achieve entanglement.<sup>5,6</sup> For QDs grown on the (001) substrate, a zero fss is hard to achieve, because piezoelectricity, interface and strain asymmetries, or even a modest QD elongation induces a lateral anisotropy leading to sizable values of the fss.<sup>7</sup> Recent advances to reduce the fss by postgrowth techniques such as thermal<sup>8</sup> or laser<sup>9</sup> annealing are inefficient, expensive, and hardly applicable on an industrial scale. Moreover, only parts of the QDs, processed in this way, actually emit entangled photon pairs after all.

Structural QD anisotropies originate from different surface mobilities along  $[110]$  and  $[1-10]$ ,<sup>10</sup> which are tied to the orientation of the underlying zinc-blende lattice with respect to the (001) substrate. Moreover, piezoelectric fields,<sup>11-13</sup> and anisotropies of strain and interfaces arise. This leads to a reduction in the carrier confinement symmetry to  $C_{2v}$  or lower and is an intrinsic characteristic of the (001)-substrate orientation.

Therefore, we propose to abandon this orientation and turn to the (111) substrate for QD growth. None of the above-mentioned effects arise on this surface. From the investigations in Refs. 14 and 15 we expect an at least threefold rotational symmetry of the QD structure. The first goal

of this Rapid Communication is to show that the corresponding piezoelectric field does not lower this symmetry any further. In effect the excitonic bright states remain degenerate and an intrinsically perfect source of entangled photon pairs is available. This result is of general character for this surface and applies to all self-organized QDs in the zinc-blende system. Using eight-band  $\mathbf{k}\cdot\mathbf{p}$  calculations in conjunction with the configuration-interaction (CI) method,<sup>16,17</sup> we illustrate this result by comparing the piezoelectric fields and excitonic properties for lens-shaped QDs, grown on the (001) and on the (111) substrates. Throughout this Rapid Communication, the (111) substrate refers to the As terminated (111)B surface.

Apart from the zero bright splitting, the spectroscopic separability of excitonic and biexcitonic emissions is essential. Therefore, the second goal is to analyze the biexciton binding energy as a function of QD size, (vertical) aspect ratio, and composition.

Third, we investigate the role of the second-order piezoelectric field with respect to these structural variations. For pure (111)-InAs QDs a reversal of the (net) built-in piezoelectric field is observed, which inverses the vertical electron-hole alignment. Since the importance of the second-order piezoelectric effect is still under discussion,<sup>12,13,18,19</sup> the measurement of the electron-hole dipole, e.g., utilizing the Stark shift [see Fry *et al.*<sup>20</sup> for (001)-In(Ga)As QDs] could shed more light into this issue. Vice versa, since the orientation of the built-in piezoelectric field depends on the composition of the QD, those measurements can deliver information on this property.

The piezoelectric field and its orientation for (111)-grown QDs are of large interest (i) first in view of its impact on the lateral symmetry of the confinement potential and (ii) second with respect to the field distribution in vertical direction,

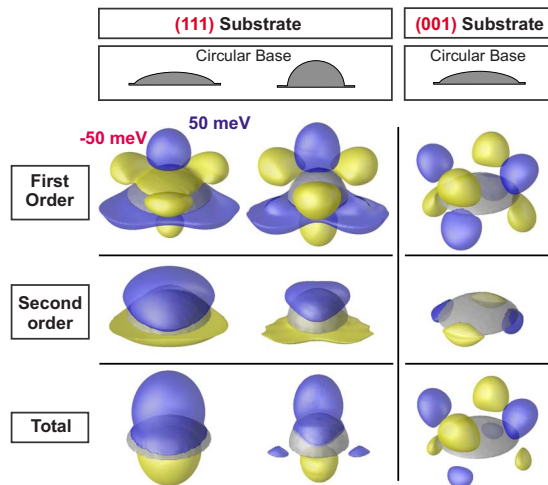


FIG. 1. (Color online) Comparison of the piezoelectric fields (first and second orders) for QDs grown on (111)B substrate to those grown on (001). Isosurfaces are shown for values of 50 meV (blue/gray) and  $-50$  meV (yellow/light gray), respectively.

the corresponding electron-hole alignment, and the related few-particle binding energies.

(i) To compare the impact of the substrate orientations on the piezoelectric potential (Fig. 1) lens-shaped QDs are chosen as model system: for the (111)-grown QDs, the potential shows  $C_{3v}$  symmetry and a strong gradient along the growth direction, in contrast to the (001)-grown counterpart, with only  $C_{2v}$  in-plane symmetry and no significant potential drop along the [001] axis. The field distribution of the (111)-grown QD is similar to the one of  $c$ -plane wurtzite-type GaN/AlN or InN/GaN QDs.<sup>21–23</sup> The magnitude of the potential drop, however, is much larger for the nitride QDs and the field is additionally superposed by pyroelectric effects, which do not occur in zinc-blende crystals.

(ii) The orientation of the piezoelectric field in growth direction results from a subtle interplay between first- and second-order piezoelectric effects. The importance of second-order effects was first discovered for (111)-In(Ga)As/GaAs quantum wells (QWs),<sup>18</sup> where the first-order piezoelectric fields alone were found to be not sufficient to explain a number of Stark-shift measurements:<sup>24–27</sup> at larger strain the nonlinear piezoelectricity starts to take effect. It provides, however, only a small but significant contribution in the quantum well system, because the maximal In concentration in In(Ga)As QWs can hardly exceed  $\approx 20\%$ . Piezoelectric constants are taken from Ref. 18.

In QDs, much larger In concentrations (up to 100%) can be achieved, which consequently leads to a large strain inside the QDs. As a result, nonlinear piezoelectric effects cannot be neglected in QDs. As can be seen in Fig. 1 for (001)-grown InAs QDs (Fig. 1, right), first- and second-order effects compensate each other inside the QD,<sup>12</sup> whereas in (111)-grown InAs QDs (Fig. 1, left and center), the second-order contributions are clearly dominant and therefore determine the orientation of the piezoelectric field.

The single-particle electronic states are calculated using a true three-dimensional implementation of the eight-band  $\mathbf{k} \cdot \mathbf{p}$  envelope-function method,<sup>13,28</sup> accounting for different dot

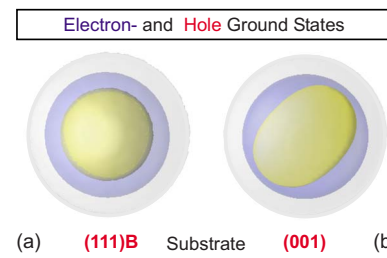


FIG. 2. (Color online) Orientation of electron (blue/gray) and hole (yellow/light gray) wave functions for a lens-shaped QD on two substrate orientations.

sizes, shapes, and composition profiles, for the inhomogeneous strain distribution, piezoelectricity, and band-coupling and -mixing effects. The main differences between the two substrate orientations are the missing electron  $p$ -state splitting and a vertical charge separation depending on the balance of first- and second-order piezoelectric terms for a given composition for (111) QDs. Energy shifts occur due to different strain field distributions for changing substrates.<sup>29</sup>

The excitonic fine-structure splitting in QDs, although a two-particle effect, results from a distortion of electron and/or hole ground state below  $C_{3v}$  symmetry.<sup>7</sup> Such a distortion can originate from QD elongation, inequivalent side facets, or piezoelectric fields.<sup>7</sup> The role of the latter is illustrated in Fig. 2. For a (001)-grown lens-shaped QD [Fig. 2(b)] the hole ground state is elongated along [110] whereas, in the case of a (111)B-grown QD [Fig. 2(a)], electron and hole ground states show no deformation in any lateral direction.

An important peculiarity of (111) QDs is the vertical distribution of the piezoelectric field inside the QD and its influence on the vertical position of electron and hole states (Fig. 3). In the case of zero piezoelectric field the electron center of mass lies above that of the hole [Figs. 3(a) and 3(b)]. This is well known from (001)-pyramidal QDs and related to a subtle interplay between the QD shape and strain.<sup>30</sup> Taking into account first-order piezoelectricity enhances the dipole by pulling the hole center of mass down to the QD bottom [Figs. 3(c) and 3(d)]. The electron state moves up less pronounced than the hole state, because its smaller effective mass makes it more “resistant” against small potential changes. Adding second-order piezoelectric effects, however, reverses the picture completely [Figs. 3(e) and 3(f)]. The electron state moves down and the hole state moves up. Consequently the direction of the dipole changes. Along, the vertical extension of the hole state increases drastically. For QDs with a large aspect ratio (Fig. 3, right), electron and hole wave functions are almost identical in size and shape.

The few-particle properties such as fine-structure splitting and biexciton binding energies are calculated using the CI model,<sup>16,17</sup> thus taking into account direct Coulomb interaction, exchange—including dipole-dipole terms—and large parts of correlation effects. In Fig. 4 the calculated values of the fine-structure splitting as functions of the QDs vertical aspect ratio are shown for the (111) substrate orientation. For (001) QDs (Refs. 12 and 13) fss values of several tens of

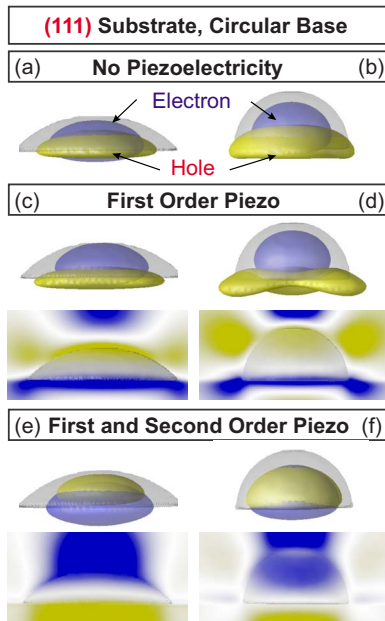


FIG. 3. (Color online) The position of electron and hole ground-state wave functions (isosurfaces at 65% probability density) dependent on the vertical aspect ratio and the order of the piezoelectric field. For (c)–(f) vertical slices of the piezoelectric potential are shown.

$\mu\text{eV}$  are found due to the symmetry breaking effect of piezoelectricity. By contrast the (111) QDs exhibit no fss at all as expected from our symmetry considerations. This result can only be reproduced for the (001) QDs if the piezoelectric potential is artificially removed from our calculations.

Symmetry lowering effects due to the atomistic nature of the QD interface and such atomistic symmetry anisotropies that are not captured by the inclusion of piezoelectricity are not part of our model. For the (111) QDs, however, such effects are not expected to lower the symmetry below  $C_{3v}$ . Hence, the fss still remains zero for (111) QDs. Only random alloying effects within the QD for InGaAs(111) QDs can lead to a deviation from the zero fss.<sup>31</sup>

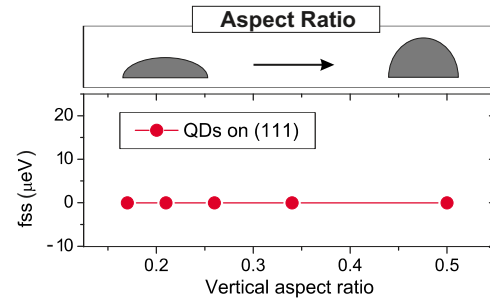


FIG. 4. (Color online) The exciton bright splitting as a function of vertical aspect ratio for lens-shaped InAs/GaAs QDs.

The vertical positions of electron and hole wave functions along with their lateral extensions determine the Coulomb interaction within excitonic complexes such as the ground states of exciton ( $X$ ) or biexciton ( $XX$ ) and the biexciton binding energy  $\Delta E(X, XX) = \omega(X \rightarrow 0) - \omega(XX \rightarrow X)$ . The latter is particularly important, because large values of  $\Delta E(X, XX)$  permit the spectral separation of  $X$  and  $XX$  emissions.

As the vertical position of the charge carriers is predominantly determined by the balance of first- and second-order piezoelectric field effects and the fields, in turn, by the QD size, shape, and chemical composition, the biexciton binding energy is a useful quantity to gather information on the QD structure. The drop of the vertical piezoelectric field across the QD vertical extension together with the corresponding average field strength is shown in Figs. 5(a) and 5(c) as a function of QD size, vertical aspect ratio, and chemical composition. The exciton ground-state transition energy along with the respective biexciton binding energy  $\Delta E(X, XX)$  is plotted in Figs. 5(d)–5(f) and Figs. 5(g)–5(i).

The diameter of the lens-shaped QDs of the size series varies between 10.2 and 20.0 nm and the height varies between 2.1 and 4.2 nm. The third QD of this series appears in all three series as indicated by vertical arrows in Fig. 5. Due to the quantum size effect, the exciton energies decrease with increasing QD size. The strength of the piezoelectric field remains constant across the series resulting in an increasing

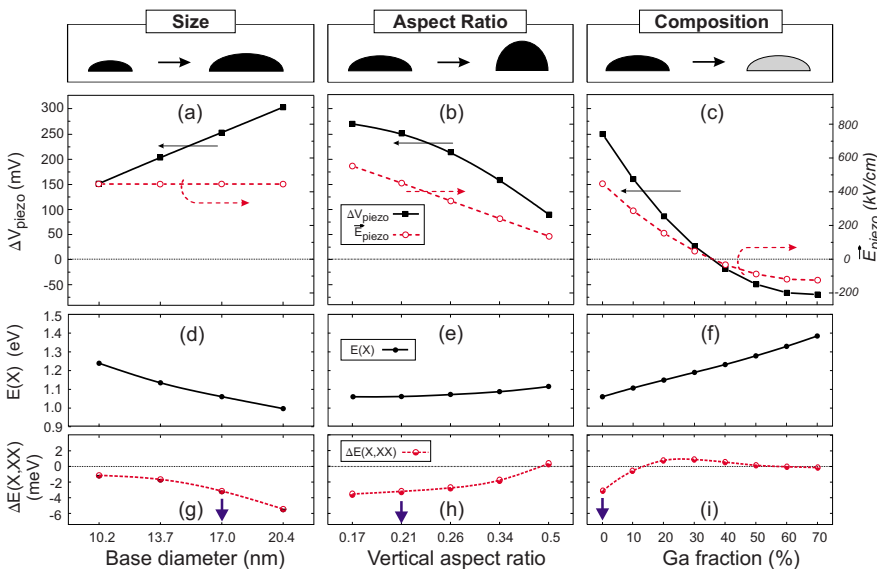


FIG. 5. (Color online) (a)–(c) Drop of the vertical piezoelectric field across the QD height at the center (black solid lines) together with the corresponding average field strength (red/gray dashed lines). (d)–(f) Exciton energy and (g)–(i) biexciton binding energy  $\Delta E(X, XX)$  as functions of size, vertical aspect ratio, and composition of (111)-grown QDs. Negative (positive) values of the  $XX$ -binding energy correspond to antibinding (binding)  $XX$  energies. Vertical arrows mark identical QDs.

vertical potential drop and a larger spatial separation of electron and hole ground states. Correspondingly, the biexciton binding energy decreases from  $-1$  meV for small dots to about  $-6$  meV for large QDs.

The aspect ratio of the second series varies between 0.17 and 0.5, while their volume is preserved. In contrast to the first series, a *decrease* in the field strength with increasing QD height is observed along with a decrease in the potential drop. The electron-hole charge separation decreases; thus, the biexciton binding energy rises.

In the last series the Ga content has been varied between 0% and 70%. For Ga fractions above 70% the lattice mismatch is not sufficient for strain-driven QD formation. The strain inside the QDs decreases for lower In concentrations. Hence, the second-order piezoelectric field strength diminishes rapidly and the first-order field component becomes dominant. Since the latter points in opposite direction, the resulting piezoelectric field reverses its orientation with a turning point in between 30% and 40%. The charge separation is minimal at this point (plus a small offset due to the strain inhomogeneity) and, hence, the biexciton binding energy becomes maximal. Consequently, the In/Ga ratio of the QD is the decisive parameter for the spectral separation of exciton and biexciton ground-state emissions.

In conclusion, due to the threefold rotational symmetry of the (111) surface QDs with  $C_{3v}$  symmetry or higher are expected to develop during growth. In contrast to QDs on

(001)-oriented substrates, the symmetry of the confinement potential of (111) QDs is not lowered by piezoelectric effects. As a result the excitonic bright splitting vanishes and the  $XX \rightarrow X \rightarrow 0$  recombination cascade can be used for the generation of entangled photons. The only remaining source of a small fine-structure splitting is random alloying effects for ternary InGaAs QDs.

The piezoelectric field in (111) QDs predominantly points toward the growth direction and gives rise to a vertical charge separation. First- and second-order fields are oriented in opposite directions. The In/Ga ratio inside the QD determines the leading contribution of the piezoelectric field and can be employed to compensate both terms in order to achieve a field-free situation with maximal electron-hole overlap. The biexciton binding energy depends on the net piezoelectric potential drop across the QD vertical extension and becomes maximal if the first- and second-order fields outweigh each other within the QD interior. By choosing the proper size, shape, and chemical composition it is possible to design a QD with a large spectral separation of exciton and biexciton.

Fruitful discussions with U. Pohl, V. Haisler, and S. Rodt are acknowledged. This work was supported by Deutsche Forschungsgemeinschaft in the frame of SFB 787. The calculations were performed on a IBM p690 supercomputer at the HLRN Berlin/Hannover.

\*andrei@sol.physik.tu-berlin.de

- <sup>1</sup>A. Schliwa, M. Winkelkemper, and D. Bimberg, German Patent Application No. 10 2008 036 400.2 (2008).
- <sup>2</sup>E. Knill, R. Laflamme, and G. J. Milburn, *Nature (London)* **409**, 46 (2001).
- <sup>3</sup>A. Shields, *Science* **297**, 1821 (2002).
- <sup>4</sup>O. Benson, C. Santori, M. Pelton, and Y. Yamamoto, *Phys. Rev. Lett.* **84**, 2513 (2000).
- <sup>5</sup>N. Akopian, N. H. Lindner, E. Poem, Y. Berlatzky, J. Avron, D. Gershoni, B. D. Gerardot, and P. M. Petroff, *Phys. Rev. Lett.* **96**, 130501 (2006).
- <sup>6</sup>R. M. Stevenson, R. J. Young, P. Atkinson, K. Cooper, D. A. Ritchie, and A. J. Shields, *Nature (London)* **439**, 179 (2006).
- <sup>7</sup>R. Seguin, A. Schliwa, S. Rodt, K. Pötschke, U. W. Pohl, and D. Bimberg, *Phys. Rev. Lett.* **95**, 257402 (2005).
- <sup>8</sup>R. Seguin *et al.*, *Appl. Phys. Lett.* **89**, 263109 (2006).
- <sup>9</sup>A. Rastelli, A. Ulhaq, S. Kiravittaya, L. Wang, A. Zrenner, and O. Schmidt, *Appl. Phys. Lett.* **90**, 073120 (2007).
- <sup>10</sup>A. Kley, P. Ruggerone, and M. Scheffler, *Phys. Rev. Lett.* **79**, 5278 (1997).
- <sup>11</sup>M. Grundmann, O. Stier, and D. Bimberg, *Phys. Rev. B* **52**, 11969 (1995).
- <sup>12</sup>G. Bester, A. Zunger, X. Wu, and D. Vanderbilt, *Phys. Rev. B* **74**, 081305(R) (2006).
- <sup>13</sup>A. Schliwa, M. Winkelkemper, and D. Bimberg, *Phys. Rev. B* **76**, 205324 (2007).
- <sup>14</sup>C. Lobo and R. Leon, *J. Appl. Phys.* **83**, 4168 (1998).
- <sup>15</sup>Y. Sugiyama, Y. Sakuma, S. Muto, and N. Yokoyama, *Appl. Phys. Lett.* **67**, 256 (1995).

- <sup>16</sup>M. Brasken, M. Lindberg, D. Sundholm, and J. Olsen, *Phys. Rev. B* **61**, 7652 (2000).
- <sup>17</sup>A. Schliwa, M. Winkelkemper, and D. Bimberg, *Phys. Rev. B* **79**, 075443 (2009).
- <sup>18</sup>G. Bester, X. Wu, D. Vanderbilt, and A. Zunger, *Phys. Rev. Lett.* **96**, 187602 (2006).
- <sup>19</sup>M. A. Migliorato, D. Powell, A. G. Cullis, T. Hammerschmidt, and G. P. Srivastava, *Phys. Rev. B* **74**, 245332 (2006).
- <sup>20</sup>P. W. Fry *et al.*, *Phys. Rev. Lett.* **84**, 733 (2000).
- <sup>21</sup>A. D. Andreev and E. P. O'Reilly, *Appl. Phys. Lett.* **79**, 521 (2001).
- <sup>22</sup>M. Winkelkemper, A. Schliwa, and D. Bimberg, *Phys. Rev. B* **74**, 155322 (2006).
- <sup>23</sup>M. Povolotskyi, A. D. Carlo, and S. Birner, *Phys. Status Solidi C* **1**, 1511 (2004).
- <sup>24</sup>R. A. Hogg *et al.*, *Phys. Rev. B* **48**, 8491 (1993).
- <sup>25</sup>J. L. Sanchez-Rojas, A. Sacedon, F. Gonzalez-Sanz, E. Calleja, and E. Munoz, *Appl. Phys. Lett.* **65**, 2042 (1994).
- <sup>26</sup>C. H. Chan, M. C. Chen, H. H. Lin, Y. F. Chen, G. J. Jan, and Y. H. Chen, *Appl. Phys. Lett.* **72**, 1208 (1998).
- <sup>27</sup>S. Cho, J. Kim, A. Sanz-Hervas, A. Majerfeld, G. Patriarche, and B. Kim, *Phys. Status Solidi A* **195**, 260 (2003).
- <sup>28</sup>O. Stier, M. Grundmann, and D. Bimberg, *Phys. Rev. B* **59**, 5688 (1999).
- <sup>29</sup>V. Mlinar and F. Peeters, *Appl. Phys. Lett.* **91**, 021910 (2007).
- <sup>30</sup>W. Sheng and J. P. Leburton, *Phys. Rev. B* **63**, 161301(R) (2001).
- <sup>31</sup>V. Mlinar and A. Zunger, *Phys. Rev. B* **79**, 115416 (2009).